Immunogenomic-based analysis of hierarchical clustering of diffuse large cell lymphoma

Longhao Wang
First Affiliated Hospital of Zhengzhou University
Wei Yuan
People'Hospital of Zhengzhou
Lifeng Li
First Affiliated Hospital of Zhengzhou University
Zhibo Shen
First Affiliated Hospital of Zhengzhou University
Qishun Geng
First Affiliated Hospital of Zhengzhou University
Yuanyuan Zheng
First Affiliated Hospital of Zhengzhou University
Jie Zhao (Jiezhaoz2016@163.com)
First Affiliated Hospital of Zhengzhou University

Research Article

Keywords: genomic profiling, immune subtypes, IRF4, prognosis, DLBCL

Posted Date: April 11th, 2022

DOI: https://doi.org/10.21203/rs.3.rs-1530280/v1

Immunogenomic-based analysis of hierarchical clustering of diffuse large cell lymphoma

Longhao Wang[1,2#], Wei Yuan[3,4#], Lifeng Li[1], Zhibo Shen[1,2], Qishun Geng[1,2], Yuanyuan Zheng[1,2], Jie Zhao[1,2*]

[1] Internet Medical and System Applications of National Engineering Laboratory, [2] Department of Pharmacy, The First Affiliated Hospital of Zhengzhou University, [3] People's Hospital of Henan University of Chinese Medicine, [4] People'Hospital of Zhengzhou, Zhengzhou 450052, Henan, China.

# These authors contributed equally to this work.

* Correspondence: zhaojie: zhaojie@zzu.edu.cn

Longhao Wang: longhaowang@163.com

Wei Yuan: zzyuanwei@qq.com

Lifeng Li: lilifeng0317@163.com

Zhibo Shen: shenzhibo233@163.com

Qishun Geng: 18845893725@163.com

Yuanyuan Zheng: anyuan0315@gmail.com

Jie Zhao：zhaojie@zzu.edu.cn

Abstract

Diffuse Large B cell lymphoma (DLBCL) is one of the most usual type of adult lymphoma with heterogeneousness in histological morphology, prognosis and clinical indications. Prior to this, several studies were carried out to determine the DLBCL subtype based on the analysis of the genome profile.However, classification based on assessment of genes related to the immune system has limited clinical significance for DLBCL. We systematically explored the DLBCL gene expression dataset and provided publicly available clinical information on patients with GEO and TCGA. In this research, 928 DLBCL samples from the Cancer Genome Atlas (TCGA) were applied, we calculated 29 immune-related genomes' enrichment levels in each sample and stratified them into high immunity that was based on ssGSEA score (Immunity_H, n=323,68.7%), moderate (Immunity_M, n= 135, 28.7%) and low (Immunity_L, n= 12,2.6%). The ESTIMATE algorithm was used to calculate matrix score (range: -1,800.51,901.99), immunity score (range: -1,476.28,780.33), estimated score (range: -2,618.28,098.14), and tumor purity (range:0.216 0.976), All of them were significantly correlated with immune subtypes (Kruskal Wallis test, $P < 0.001$). At the same time, the correlation of related genes was analyzed by immunohistochemistry staining. In addition, DLBCL cells were cultured in transfected and vitro with siRNA to verify correlation analysis and gene expression. Finally, human peripheral blood lymphocytes were incubated with DLBCL cells, and stained. Flow cytometry was applied to analyze genes' influence on immune function.By analysis, immune checkpoint and HLA gene expression levels were higher in the Immunity_H group (Kruskal Wallis test, $P < 0.05$). The levels of Tfhs (follicular helper T cells), Monocytes, $CD8^+$ T cells, M1 Macrophages, M2 Macrophages, $CD4^+$ memory activated T cells, were the most excellent in Immunity_H, and total survival rate was higher in the Immunity_L. The GO term discovered in Immunity_H is connected with immunity. Through analysis, IRF4 (MUM1) was identified by us as immunotherapeutic target and a potential prognostic marker for DLBCL, which was made sure by using molecular biology experimentations. To conclude, immunosignature made a connection between DLBCL subtypes play a position in DLBCL prognostic stratification. Immunocharacteristics-related DLBCL subtypes' construction predicts expected patient results and supplies conceivable immunotherapy candida.

Keywords: genomic profiling, immune subtypes, IRF4, prognosis, DLBCL

Introduction

Lymphoma is the fourth ahead cause of cancer deaths in the United States and one of the most common cancers. DLBCL accounts for approximately one-third of lymphoma's all instances world-wide[1]. Two molecularly different DLBCL's shapes have been identified through gene expression patterns including germinal center B-cell-like (GCB) types and activated B cell-like (ABC)[2]. The immunohistochemical expression (IHC) of CD10, IRF4/MUM1 and Bcl-6 have been used to categorize DLBCL's examples into non-GCB groups and GCB. Relevant researches have revealed that IRF4's overexpression is connected with patients' miserable prognosis with DLBCL. In spite of the variety of clinical, morphologic and molecular human malignancies used to be classified by parameters nowadays, DLBCL patients' 40% survival continues to be poor.

Up till the present moment, there are few treatment alternatives for DLBCL. Immunotherapy is a new treatment that improves the survival prospects of DLBCL patients, including the blocking of immune checkpoints. [3]. In spite of the fantastic advance in immunotherapy strategies, favourable

effects, nevertheless, have been demonstrated merely in a subset of patients. Immunotherapy's responsiveness is influenced by Definite factors, for example, host germline genetics, PD-L1 grades and tumour genomics. [4, 5]. It has been discovered that tumor microenvironmental heterogeneousness can be used as biomarkers for prognosis and immunotherapy sensitivity of various kinds of cancers. [6, 7]. It is noteworthy that both tumor-associated stromal cells and infiltrating immune cells are significant components of tumor immune microenvironment and drama a significant part in tumor development, progression, and drug opposition. [8, 9]. In consequence, an increasing number of researches are concentrating on these factors, supplying fresh perceptions into the prognostic value and therapeutic methods of tumor biology.

In our research, based on immune genomic analysis, patients were divided with DLBCL into three groups: Immunity_L, Immunity_M and Immunity_H. A strong connection has been demonstrated by us between categorization and immune infiltration and survival results. The construction of immune signatures that are associated with DLBCL subtypes may contribute to the search for prognostic markers and novel immunotherapy marks.

Materials and methods

Data source

DLBCL patient of gene expression and clinical data were downloaded from Gene Expression Omnibus (GEO) database. In this research, clinical data that were related to age, stage, subtype, LDH, IPI, ECOG and survival were collected by us from GEO, and a total of 928 DLBCL patients were enrolled.

Hierarchical cluster analysis of DLBCL

29 immune-related gene sets were applied by us, including 707 genes, depicting different immune cell types, pathways and functions. The enrichment grades of immune biosignatures were worked out by using single sample gene set enrichment analysis (ssGSEA), as demonstrated in former learnings[10], and quantified typical immune cell sorts, roles, and pathways. DLBCL was hierarchically clustered by using unsupervised learning approach and further divided into Immunity_M, Immunity_L and Immunity_H that be based on immune score.

Calculation of the immune and stromal scores and Estimation of the CIBERSORT

ESTIMATE is an approach to infer tumor purity's fraction by using immune cells and stromal cells in malignancy tissue applying expression data. In the light of the Immunity_H, Immunity_M and Immunity_L groups, ESTIMATE algorithm was applied to estimate the immune grade and stromal grade and ESTIMATE DLBCL patients' score. We used deconvolution strategies to calculate parts of 22 human immune cell types. This is a biological method of cell-type Identification through estimation Relative Subsets of RNA Transcripts (CIBERSORT). The CIBERSORT package was applied to calculate immune cell types' distribution in each subset, and immune cell's proportion types in DLBCL's subtypes was compared by Kruskal-Wallis test[11].

GO and KEGG pathway enrichment analysis

GSEA package was used to analyze gene aggregation and enrichment in DLBCL patients. Gene Ontology (GO) and The Kyoto Encyclopedia of Genes Genomes (KEGG) analyses were used to evaluate the differentially expressed genes' functional function between Low and High group[12]. Differential gene set enrichment was examined using the limma R package. $P < 0.05$ was used as the cut-off value.

Survival analyses

The Kaplan–Meier survival curve was drawn based on the patient's survival information to visualize the survival difference between immune subtypes.

Cell lines and Cell culture

Human peripheral blood lymphocytes and DLBCL cell line DS (obtained from ATCC) were cultured in RMPI 1640 medium (Gibco, USA) supplemented with 10% fetal bovine serum (FBS, Gibco, USA), streptomycin and penicillin in 5% CO_2 humidified chamber, at 37℃.

Using siRNA to interfere with gene expression

DS cells were transfected with synthetic siRNA oligonucleotides (concentration:100nmol/L). Lipofectamine 8000 (Beyotime, China) was used, by Gene Pharma (Gene Pharma, Shanghai, China) [13]. The sequence of siRNA is as follows: siIRF4: 5′ -GGACACACCUAUGAUGUUAUU-3′ ; and siControl, 5′ -UAAGGCUAUGAAGAGAUACUU-3′ [14].

RNA extraction and Quantitative Real-time PCR

DLBCL cells were inoculated into transfected and cell culture dishes with siRNA oligonucleotide. After transfection with siIRF4 or control siRNA for 48 h. PrimeScript™ RT Kit with gDNA Eraser (CAT. No. RR047A, Takara, Dalian, China) was reversed transcription following instructions of manufacturer. After transcription, cDNA was quantitatively analyzed applying QuantiNova™ SYBR Green PCR kit (Cat.No.208054, QIAGEN, Germany) and real-time PCR system (Applied Biosystems, Foster City, Calif), pursuant to instructions of the producer. For each sample, the mRNA abundance was normalized to the quantity of GAPDH. Primers are as follows: IRF4： Forward, 5 '- CTACACCATGACAACGCCTTACC - 3' and reverse, 5-GGCTGATCCGGGACGTAGT -3'. GAPDH: Forward, 3' - AAAGGGTCATCATCTCTG -5', reverse,5 '- GCTGTTGTCATACTTCTC - 3'.

Western blotting assay

DLBCL was inoculated into cell culture dishes and transfected with siControl and siIRF4 oligonucleotides respectively. After 48 h, cells were collected and lysed with cell lysate for Western blotting analysis. BCA assay was used to determine protein concentration, and primary antibody was used: anti-IRF4(Cat. No.62834), anti-PD-L1(Cat. No.13684), (Cell Signaling Technology, Inc., Boston, MA). The primary antibody was diluted at 1:1000 and incubated overnight (12-18h) at 4℃. And wash with TBST (Tris Buffer Saline Tween-20) 4 times, 5 minutes each time. Incubate with peroxisase-labeled 1:5000 or secondary peroxisase-labeled goat anti-mouse IgG diluted ZGSBBio, Inc., China) for 2 hours at room temperature. ECL kit (Beyotime, China) was applied for membrane detection. All proteins were loaded with GAPDH as control.

Flow cytometry analysis

We directly incubated cells with fluorescent-labeled antibodies and performed cell fluorescence analysis using flow cytometry (BD FACS Canto) to ascertain cell phenotypes for assessment. CD8 and PD-L1 can be stained straight on the cell surface and discovered, while granular enzyme B and IFN- γ are employed for intracellular staining, so cells are foremost immobilized with 4%

paraformaldehyde for 20-30min, then stained with fluorescent-pigment-labeled antibodies and incubated in dark ice for 15 min. Antibody choice FITC- conjugated anti- Granzyme B antibodies and Anti-IFN- γ were stained with PE-conjugated anti-PD-L1, PE-Cy7 conjugated anti-CD8, and APC conjugated cells (BD, USA).

Immunohistochemistry (IHC) staining of human diffuse large B lymphoma tissue array

We purchased human Diffuse Large B lymphoma tissue Chip array (OD-CT-LY02-001) from Shanghai Outdo Biotech Co. Ltd. IRF4 antibody (Cat. No.62834, Cell Signaling Technology) and PD-L1 antibody (Cat. No.13684, Cell Signaling Technology) were stained by IHC to detect the expression of IRF4 and PD-L1 (1:50 dilution). Briefly, 4 μm of tissue array sections were blocked with dehydrated peroxidase. Antigen recuperation was executed at 0.01 mol/L in citrate buffer and autoclaved. The primary antibody was added and incubated overnight at 4℃. Slides were re-stained with hematoxylin. The stained slides were observed by microscopy to obtain images. IHC scoring was also performed separately to analyze the correlation between IRF4 and PD-L1.

Statistical Analysis

All statistical tests were analyzed applying R (3.5.2) and unconditional data were extracted using Fisher s or $\chi 2$ tests. A Kruskal-Wallis test and Wilcoxon test were applied for two or more uninterrupted data categories. Fisher is applied to sort relation between defined subtypes and clinical information statistically. Survival analysis was executed employing the R box survival. Kaplan-Meier curve was carried out to screen prognostic immune cell subclasses for survival data. All statistical analyses with $P < 0.05$ were considered statistically significant. GraphPad Prism8 software was applied to assess distinction between the two groups. T test was applied to compare parameters between categories*. It suggested that the distinction between the two categories was statistically meaning ($P<0.05$).

Results

Construction is modeled by immune subtype and patient clinical characteristics

In this study, we involved clinical data and gene expression profiles of 928 patients with DLBCL from the GEO database. The selected patients' clinical characteristics are summarized by Table 1. 62.2 years was the median age at diagnosis (range: 20.8-86.0), with 517 males (55.7%) and 411 females (44.3%). We conducted the study according to the scheme flow in Figure 1(FIG.1). An unsupervised cluster analysis of 29 immune-associated gene sets was foremost performed by us. There were three clear sets of samples according to the ssGSEA score of the genome: Immunity_L (n = 71, 7.7%), Immunity_M (n = 322, 34.7%) and Immunity_H (n = 535, 57.7%) (Fig.3A). As demonstrated in the heat map (Fig.2A), immunity-related genes' expression degree was more depressed in the Low group than in the High group. Stromal scores (range- 586.88 to 1982.43), immune scores (range 832.23 to 3359.60), Estimate scores (range 1387.54 to 4737.90) and tumor purity (scope 0.27 to 0.69) are revealed for patients with DLBCL. Immune scores and particular mesenchymal were worked out to forecast the level of infiltrating immune cells and mesenchymal and to provide a basis for inferring tumor purity in the tumor tissue (Fig.2B). Results demonstrated that tumor purity was importantly more down in the Immunity_H group and substantially more excellent in the Immunity_L group (Kruskal-Wallis test, $P < 0.001$), indicating that this immunotyping correlation analysis with tumor purity in DLBCL is meaningful. These consequences showed that the Immunity_L sample contained an unusually unusual amount of tumor cells, the Immunity_H sample contained an unusually high figure of immune and stromal cells, and the Immunity_M sample took an intermediate amount of tumor cells.

Survival rate was significantly correlated with immune subsets

Next, three immune subtypes' prognostic value was measured by us on patient survival. It was discovered that the survival curves of the three subgroups Immunity_H, Immunity_M and Immunity_L were statistically significantly different (p=4.396e-08). It also demonstrated that immunophenotyping was a good predictor of survival in DLBCL. Patients in Immunity_H group had the best prognosis, those in Immunity_L group had the worst prognosis, and those in Immunity_M group were in between. As shown in (Fig.3B).

Exploration of immune subtype-related markers

In addition, we also explored the connection during the expression of PD-1, PD-L1, CD3D, HIF1A, and IRF4 genes and immune subgroups. These results showed that the expression of PD-1, PD-L1, CD3D, HIF1A, IRF4 and other genes were meaningfully different in both Immunity_H and Immunity_L groups (ANOVA text, $P < 0.001$), as shown in (Fig.3C-H). The results of this study strongly support that the immune microenvironment affects action of immune checkpoint inhibitors in cancer patients, and it also sounds an alarm for the development of new immune checkpoint inhibitors, which cannot ignore the important role of immune microenvironment in novel immunotherapy.

HLA genes were meaningfully correlated with immune subsets

To test immune-related genes' expression in each subgroup, HLA genes' expression is then explored by us in three immune subgroups. "* * *", "* *", "*", "ns" respectively based on one-way ANOVA ($p < 0.001$, $p < 0.01$, $p < 0.05$ and $p < 1$. These consequences demonstrated that HLA family genes' expression in the Immunity_H was importantly more excellent than that in Immunity_M and Immunity_L, and it was the most down in Immunity_L(Fig.4A). Among 24 HLA-related genes, only hLA-G, HLA-DRB6, HLA-DPB2, HLA-DOB and HLA-B genes had no significance in immune subgroup distribution. The distribution of other HLA family members in immune subgroup was statistically significant ($P <0.05$).

Immune subtypes were correlated with immune cell infiltration importantly

To further investigate the important function of tumor microenvironment in DLBCL, the ratio of 22 human immune cell subsets in DLBCL was assessed using the CIBERSORT package in R software. The results revealed that Monocytes, M1 Macrophages, M2 Macrophages, CD8+ T cells, CD4+ memory activated T cells and follicular helper T cells were importantly high up in Immunity_H than Immunity_L and the consequences of B cells naive, B cells memory, plasma cells, CD4+ naive T cells in Immunity_H groups and Immunity_M were importantly more down than the Immunity_L group (Fig.4B).

KEGG enrichment analysis and GO

Based on the improvement scores in each sample, the differential genes in the Immunity_L and Immunity_H groups were screened. (Fig.4C) shows correlation to the best 5 pathways with the most excellent GO and (Fig.4D) reveals the highest 5 pathways with the most excellent KEGG correlation. KEGG analysis showed that the differential genes in Immunity_H and Immunity_L groups were mainly enriched in GO analysis showed that Low group differential genes and High group were improved with immune synapse formation substantially, positive regulation of interleukin-2 biosynthetic process, positive regulation of nitric oxide synthase biosynthetic process, regulation of

tolerance induction, T cell receptor signaling pathway, regulation of tolerance induction, and T-cell receptor complexes.

PD-L1 regulates IRF4 expression in DLBCL.

We then valued the expression of PD-L1 proteins and IRF4 by using immunohistochemistry (IHC) in 30 patients diagnosed with DLBCL (Table 1). IRF4 expressions and PD-L1 were notably discovered in the majority of examples in this cohort, whereas PD-L1 overexpression was substantially more usual in cases with excellent IRF4(Fig.5A). PD-L1 IHC score had a good correlation with IRF4 score ($P < 0.001$, Fig.5B). Finally, immunoblotting（Fig.5C) and real-time quantitative PCR (Fig.4D) detection confirmed that knockdown of IRF4 expression in DLBCL could effectively inhibit PD-L1 expression.

Effect of IRF4 on immune function

In this study, we observed that knocking down IRF4 resulted in reduced PD-L1 induction, and IFN-γ induction further confirmed the correlation between IRF4 and PD-L1 (Fig.6A-B). Compared with the control group, DS cells with knockdown IRF4 were co-incubated with PBMC, and the immune function of CD8+ T cells was detected by using flow cytometry. It was observed that the production of IFN-γ and Granzyme B related molecules of CD8+ T cells was more excellent than that of the control group (Fig.6C). At the same time, we found that compared to the control group. Knocking down IRF4 can inhibit the differentiation of CD4+ T cells into Treg (Fig.6D).

Discussion

Despite the wide variety of clinical, morphological and molecular parameters used to classify DLBCL today, the 40% survival rate remains poor [15, 16]. Currently, Genome mapping has been used to identify and diagnose diverse cancers' molecular subtypes, and an amount of evidences that the tumor microenvironment plays an significant part in tumgenesis, development and treatment[17, 18]. In the meanwhile, immune cells and stromal cells in tumor microenvironment also play a significant part in prognosis at the same time and tumor progression[19, 20]. Therefore, immune-related hierarchical clustering is used to better assess patient outcomes and select therapies that are effective only for specific subtypes of DLBCL.

In our study, we calculated 928 DLBCL samples using ssGSEA and analyzed the enrichment levels of 29 immune-related genomes in each sample. Next, we used unsupervised clustering, which could be clearly based on the three DLBCL subtypes identified by the ssGSEA score: Immunity_High subtype, Immunity_Medium subtype, and Immunity_Low subtype. We used estimation algorithms to calculate each patient's score of immune, stromal and tumor purity. Analysis showed that of the three subtypes, Immunity_High was connected with importantly more excellent prognosis and accommodated more stromal cells and immune cells than the other groups, showing increased activity in this subgroup. In addition, we discovered the expression of PD-1, PD-L1, CD3D, HIF1A, and IRF4 genes were substantially different in both Immunity_L groups and Immunity_H (ANOVA text, $P < 0.001$).

Class L human leukocyte antigen is an intracellular peptide that can be recognized by T cells on the cell surface. Changes in the HLA gene may alter the ability to express neoantigens and thus affect immune escape. Numerous studies have shown that HLA alterations are strongly associated with cancer prognosis and treatment. In our research, HLA family genes' expression was importantly higher in Immunity_H than in Immunity_L and Immunity_M.

At the same time, an increasing number of researches have illustrated a correlation between the treatment responsiveness and prognosis of tumor patients and the level of immune cell infiltration [21]. We used the CIBERSORT package in R software to evaluate 22 human immune cell subpopulations'

part in DLBCL. We discovered significant differences in the level of immune cell infiltration and the proportion of immune infiltrating cell types by immune subtype grouping through our analysis[22]. For instance, the highest proportions of CD8+ T cells and CD4+ memory T cells were discovered in Immunity_H. Meanwhile, immune checkpoints' role is to exert anti-tumor impacts by increasing the role of CD4+ T and CD8+ T cells [23, 24]. It has been reported in the past that CD8+ T cell infiltration degrees are positively correlated with cancer prognosis after immunotherapy in various kinds of solid tumors. We found by further study that Monocytes, M1 Macrophages, M2 Macrophages, CD8+ T cells, CD4+ memory activated T cells and the follicular helper T cells were meaningfully high up in Immunity_H than These consequences of B cells naive, B cells memory, Plasma cells, CD4+ naïve were meaningfully high up in Immunity_L than in Immunity_H and Immunity_M. Besides, the CD8+ /Treg ratio was considerably high up in Immunity_High than in Immunity_Low. This indicates that Immunity_High has higher immune response and stronger anti-tumor activity[25-27].

IRF4/MUM1, a member of the IRF family, is specifically expressed in lymphocytes and is involved in immune regulation through a series of signal transduction actions. Previous studies have shown that abnormal IRF4 expression can be used as a diagnostic and prognostic marker for various hematologic malignancies. IRF4 was described by Chen et al. as a negative prognostic factor for non-small cell lung cancer[28]. Our study found that IRF4 (MUM1) was an immunotherapeutic target and a potential prognostic marker for DLBCL. We first demonstrated in DLBCL that IRF4 can up-regulate the PD-L1 expression of tumor cells. What's more, on one hand the high expression of IRF4 in tumor can inhibit function of effector T cells, and on the other hand increase the proportion of immunosuppressive cells Treg, which promote the immune escape of cancer cells. Our research showed that it was possible to inhibit the expression of IRF4 in tumor cells and relieve the immunosuppressive effect to achieve the effect of treating DLBCL.

In our study, we found IRF4's expression was meaningfully high up in Immunity_H than in Immunity_M and Immunity_L; meanwhile, we verified the positive correlation between IRF4 and PD-L1 and demonstrated that IRF4 could enhance immunosuppressive effect of tumor microenvironment. These researches showed that it was possible to inhibit the expression of IRF4 in tumor cells and relieve the immunosuppressive effect to achieve the effect of treating DLBCL.

Acknowledgements

We would like to thank several anonymous reviewers for their valuable comments and suggestions to improve the quality of the paper.

Authors' Contributions

LHW, WY and LFL designed and performed the study, and ZBS wrote the original draft. YYZ revise the manuscript. QSG participated in the analysis and super.

Funding

This study was supported by Medical Science and Technology Project of Henan Province (Grant No. SBGJ202002077), Natural Science Foundation of Henan Province of China (Grant No.202300410460).

Data availability

All datasets produced for this research are involved in the article/Supplementary Material.

Conflicts of Interest

The authors declare that they have no conflict of interest.

References

1. Howlader N, Mariotto AB, Besson C, Suneja G, Robien K, Younes N and Engels EA (2017) Cancer-specific mortality, cure fraction, and noncancer causes of death among diffuse large B-cell lymphoma patients in the immunochemotherapy era. Cancer 123:3326-3334. doi: 10.1002/cncr.30739

2. Alizadeh AA, Eisen MB, Davis RE, Ma C, Lossos IS, Rosenwald A, Boldrick JC, Sabet H, Tran T, Yu X, Powell JI, Yang L, Marti GE, Moore T, Hudson J, Jr., Lu L, Lewis DB, Tibshirani R, Sherlock G, Chan WC, Greiner TC, Weisenburger DD, Armitage JO, Warnke R, Levy R, Wilson W, Grever MR, Byrd JC, Botstein D, Brown PO and Staudt LM (2000) Distinct types of diffuse large B-cell lymphoma identified by gene expression profiling. Nature 403:503-11. doi: 10.1038/35000501

3. Pascual M, Mena-Varas M, Robles EF, Garcia-Barchino MJ, Panizo C, Hervas-Stubbs S, Alignani D, Sagardoy A, Martinez-Ferrandis JI, Bunting KL, Meier S, Sagaert X, Bagnara D, Guruceaga E, Blanco O, Celay J, Martinez-Baztan A, Casares N, Lasarte JJ, MacCarthy T, Melnick A, Martinez-Climent JA and Roa S (2019) PD-1/PD-L1 immune checkpoint and p53 loss facilitate tumor progression in activated B-cell diffuse large B-cell lymphomas. Blood 133:2401-2412. doi: 10.1182/blood.2018889931

4. Havel JJ, Chowell D and Chan TA (2019) The evolving landscape of biomarkers for checkpoint inhibitor immunotherapy. Nat Rev Cancer 19:133-150. doi: 10.1038/s41568-019-0116-x

5. Sugiyama E, Togashi Y, Takeuchi Y, Shinya S, Tada Y, Kataoka K, Tane K, Sato E, Ishii G, Goto K, Shintani Y, Okumura M, Tsuboi M and Nishikawa H (2020) Blockade of EGFR improves responsiveness to PD-1 blockade in EGFR-mutated non-small cell lung cancer. Sci Immunol 5. doi: 10.1126/sciimmunol.aav3937

6. Cesano A and Warren S (2018) Bringing the next Generation of Immuno-Oncology Biomarkers to the Clinic. Biomedicines 6. doi: 10.3390/biomedicines6010014

7. Taube JM, Galon J, Sholl LM, Rodig SJ, Cottrell TR, Giraldo NA, Baras AS, Patel SS, Anders RA, Rimm DL and Cimino-Mathews A (2018) Implications of the tumor immune microenvironment for staging and therapeutics. Mod Pathol 31:214-234. doi: 10.1038/modpathol.2017.156

8. Gajewski TF, Schreiber H and Fu YX (2013) Innate and adaptive immune cells in the tumor microenvironment. Nat Immunol 14:1014-22. doi: 10.1038/ni.2703

9. Kobayashi H, Enomoto A, Woods SL, Burt AD, Takahashi M and Worthley DL (2019) Cancer-associated fibroblasts in gastrointestinal cancer. Nat Rev Gastroenterol Hepatol 16:282-295. doi: 10.1038/s41575-019-0115-0

10. He Y, Jiang Z, Chen C and Wang X (2018) Classification of triple-negative breast cancers based on Immunogenomic profiling. J Exp Clin Cancer Res 37:327. doi: 10.1186/s13046-018-1002-1

11. Newman AM, Liu CL, Green MR, Gentles AJ, Feng W, Xu Y, Hoang CD, Diehn M and Alizadeh AA (2015) Robust enumeration of cell subsets from tissue expression profiles. Nat Methods 12:453-7. doi: 10.1038/nmeth.3337

12. Yu G, Wang LG, Han Y and He QY (2012) clusterProfiler: an R package for comparing biological themes among gene clusters. OMICS 16:284-7. doi: 10.1089/omi.2011.0118

13. Wang L, Li M, Sha B, Hu X, Sun Y, Zhu M, Xu Y, Li P, Wang Y, Guo Y, Li J, Shi J, Li P, Hu T and Chen P (2021) Inhibition of deubiquitination by PR-619 induces apoptosis and autophagy via ubi-protein aggregation-activated ER stress in oesophageal squamous cell carcinoma. Cell Prolif 54:e12919. doi: 10.1111/cpr.12919

14. Yang C, He D, Yin C and Tan J (2015) Inhibition of Interferon Regulatory Factor 4 Suppresses Th1 and Th17 Cell Differentiation and Ameliorates Experimental Autoimmune Encephalomyelitis. Scand J Immunol 82:345-51. doi: 10.1111/sji.12334

15. Schmitz R, Wright GW, Huang DW, Johnson CA, Phelan JD, Wang JQ, Roulland S, Kasbekar M, Young RM, Shaffer AL, Hodson DJ, Xiao W, Yu X, Yang Y, Zhao H, Xu W, Liu X, Zhou B, Du W, Chan WC, Jaffe ES, Gascoyne RD, Connors JM, Campo E, Lopez-Guillermo A, Rosenwald A, Ott G, Delabie J, Rimsza LM, Tay Kuang Wei K, Zelenetz AD, Leonard JP, Bartlett NL, Tran B, Shetty J, Zhao Y, Soppet DR, Pittaluga S, Wilson WH and Staudt LM (2018) Genetics and Pathogenesis of Diffuse Large B-Cell Lymphoma. N Engl J Med 378:1396-1407. doi: 10.1056/NEJMoa1801445

16. Li S, Young KH and Medeiros LJ (2018) Diffuse large B-cell lymphoma. Pathology 50:74-87. doi: 10.1016/j.pathol.2017.09.006

17. Rodriguez-Ruiz ME, Vitale I, Harrington KJ, Melero I and Galluzzi L (2020) Immunological impact of cell death signaling driven by radiation on the tumor microenvironment. Nat Immunol 21:120-134. doi: 10.1038/s41590-019-0561-4

18. Wu T and Dai Y (2017) Tumor microenvironment and therapeutic response. Cancer Lett 387:61-68. doi: 10.1016/j.canlet.2016.01.043

19. Cacho-Diaz B, Garcia-Botello DR, Wegman-Ostrosky T, Reyes-Soto G, Ortiz-Sanchez E and Herrera-Montalvo LA (2020) Tumor microenvironment differences between primary tumor and brain metastases. J Transl Med 18:1. doi: 10.1186/s12967-019-02189-8

20. Rahn S, Kruger S, Rocken C, Helm O and Sebens S (2019) Response to: 'Patterns of PD-L1 expression and CD8 T cell infiltration in gastric adenocarcinomas and associated immune stroma'. Gut 68:179-180. doi: 10.1136/gutjnl-2017-315843

21. Thompson ED, Zahurak M, Murphy A, Cornish T, Cuka N, Abdelfatah E, Yang S, Duncan M, Ahuja N, Taube JM, Anders RA and Kelly RJ (2017) Patterns of PD-L1 expression and CD8 T cell infiltration in gastric adenocarcinomas and associated immune stroma. Gut 66:794-801. doi: 10.1136/gutjnl-2015-310839

22. Topalian SL, Taube JM, Anders RA and Pardoll DM (2016) Mechanism-driven biomarkers to guide immune checkpoint blockade in cancer therapy. Nat Rev Cancer 16:275-87. doi: 10.1038/nrc.2016.36

23. Sato Y, Bolzenius JK, Eteleeb AM, Su X, Maher CA, Sehn JK and Arora VK (2018) CD4+ T cells induce rejection of urothelial tumors after immune checkpoint blockade. JCI Insight 3. doi: 10.1172/jci.insight.121062

24. Farhood B, Najafi M and Mortezaee K (2019) CD8(+) cytotoxic T lymphocytes in cancer immunotherapy: A review. J Cell Physiol 234:8509-8521. doi: 10.1002/jcp.27782

25. Ali HR, Chlon L, Pharoah PD, Markowetz F and Caldas C (2016) Patterns of Immune Infiltration in Breast Cancer and Their Clinical Implications: A Gene-Expression-Based Retrospective Study. PLoS Med 13:e1002194. doi: 10.1371/journal.pmed.1002194

26. Jansen CS, Prokhnevska N, Master VA, Sanda MG, Carlisle JW, Bilen MA, Cardenas M, Wilkinson S, Lake R, Sowalsky AG, Valanparambil RM, Hudson WH, McGuire D, Melnick K, Khan AI, Kim K, Chang YM, Kim A, Filson CP, Alemozaffar M, Osunkoya AO, Mullane P, Ellis C, Akondy R, Im SJ, Kamphorst AO, Reyes A, Liu Y and Kissick H (2019) An intra-tumoral niche maintains and differentiates stem-like CD8 T cells. Nature 576:465-470. doi: 10.1038/s41586-019-1836-5

27. de Andrea CE, Schalper KA, Sanmamed MF and Melero I (2018) Immunodivergence in Metastatic Colorectal Cancer. Cancer Cell 34:876-878. doi: 10.1016/j.ccell.2018.11.012

28. Qian Y, Du Z, Xing Y, Zhou T, Chen T and Shi M (2017) Interferon regulatory factor 4 (IRF4) is overexpressed in human nonsmall cell lung cancer (NSCLC) and activates the Notch signaling pathway. Mol Med Rep 16:6034-6040. doi: 10.3892/mmr.2017.7319

Figure Legends

Table 1: Data set related information

Table 2: Detailed information of tissue array used in IHC

Figure 1: The follow diagram of this study

Figure 2: A: Based on unsupervised cluster analysis of genomic ssGSEA score, 928 DLBCL samples were divided into three groups: Immunity_H (n = 636), Immunity_M (n = 322) and Immunity_L (n = 71).B: Heat map of Immunity_H, Immunity_M and Immunity_L subtypes according to 29 immune cell types.

Figure 3: A: Analysis of differences in tumor purity between three immune subtypes. Tumor purity was importantly more down in Immunity_H group and importantly more excellent in Immunity_L (P <0.001, Kruskal-Wallis test). B: Survival analysis of three immune subgroups. The survival curves of

Immunity_L, Immunity_M and Immunity_H subgroups were significantly different (P = 4.396E-08). It also proved that immune grouping had a good predictive effect on the survival of diffuse LARGE B-cell lymphoma. Patients in Immunity_H had the best prognosis, patients in Immunity_L had got the poorest prognosis, and the Immunity_M was between them. C-H: The expression of PD-1, PD-L1, CD3D, HIF1A, IRF4 and other genes was meaningfully correlated with the immune subgroup.The expressions of PD-1, PD-L1, CD3D, HIF1A, IRF4 and other genes were meaningfully dissimilar between Immunity_L and Immunity_H (ANOVA text, P <0.001).

Figure 4: A : Immune subsets were significantly associated with HLA family genes. among 24 HLA-related genes, only five genes, HLA-G, HLA-DRB6, HLA-DPB2, HLA-DOB, and HLA-B, were not significant in the distribution of immune subsets. The remaining HLA family members were statistically distributed in the immune subgroups ($p<0.06$). B: Immune subtypes were significantly associated with immune cell infiltration.Monocytes, M1 Macrophages, M2 Macrophages, CD8+ T cells, CD4+ memory activated T cells and the follicular helper T cells were substantially high up in the Immunity_H group than in the Immunity_M groups and Immunity_L. The results of B cells naive, B cells memory, Plasma cells and CD4+ naive T cells in Immunity_L were considerably more excellent than those in Immunity_M and Immunity_H. C-D: GO and KEGG analysis Differential gene enrichment analysis of Immunity_H and Immunity_L groups.

Figure 5: A: IHC was used to detect the expression of IRF4 and PD-L1 in DLBCL. Two cases were stained with IRF4 and PD-L1 immunohistochemistry.Examine the section under a microscope. B: The images described are representative of 30 cases of DLBCL. Correlation between IRF4 IHC score and IRF4 IHC score in 30 DLBCL patients,calculated by Spearman's rank correlation methods, in 30 DLBCL cases. C: We transfected siControl and siIRF4 into DS cell line by transient transfection method. Proteins were collected and lysed, and the displayed proteins were analyzed by western blotting. D: The expression of PD-L1 was detected by real-time fluorescence quantitative PCR.The error bar represents three separate experiments.

Figure 6: A-B: PD-L1's flow cytometry analysis in siIRF4 DS cells in relation to restriction with or without IFN-γ therapy. C: Flow cytometry was used to analyze GranzyB+ CD8+ T cell or IFN-γ + CD8+ T cell frequencies. D: and CD4+T cell frequency or Treg(FOXP3) in the PBMC.

Figures

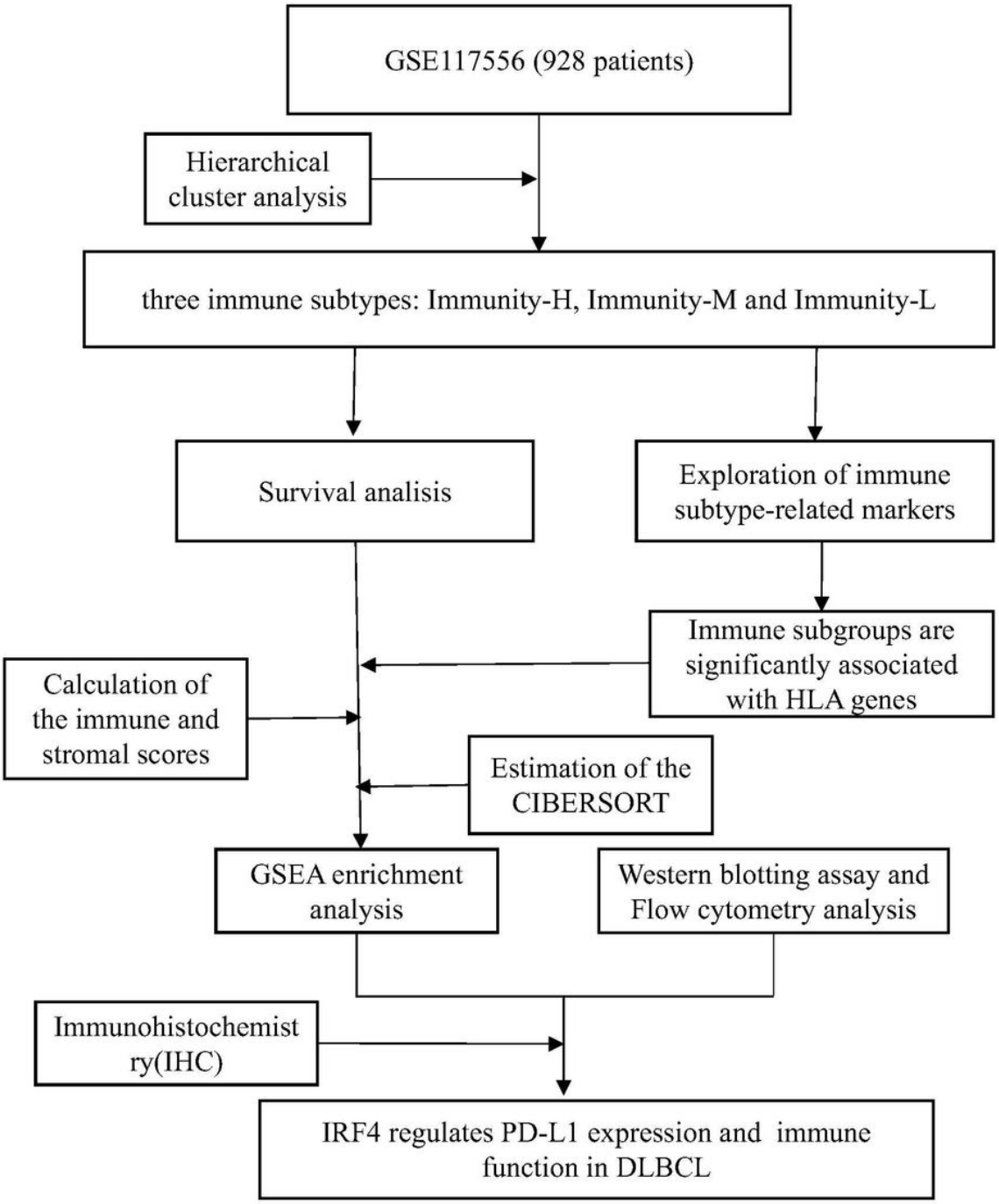

Figure 1

The follow diagram of this study

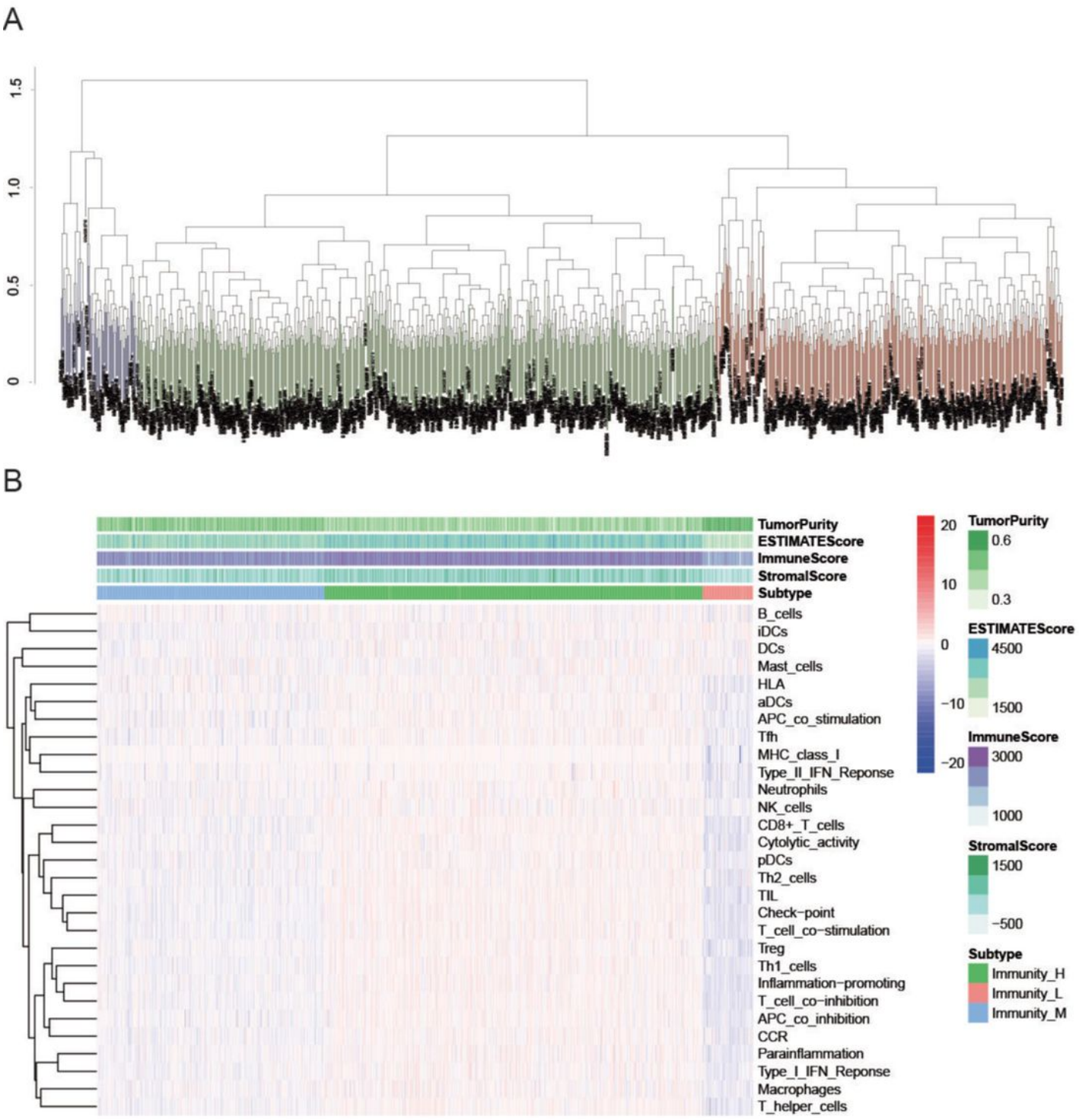

Figure 2

A: Based on unsupervised cluster analysis of genomic ssGSEA score, 928 DLBCL samples were divided into three groups: Immunity_H (n = 636), Immunity_M (n = 322) and Immunity_L (n = 71).B: Heat map of Immunity_H, Immunity_M and Immunity_L subtypes according to 29 immune cell types.

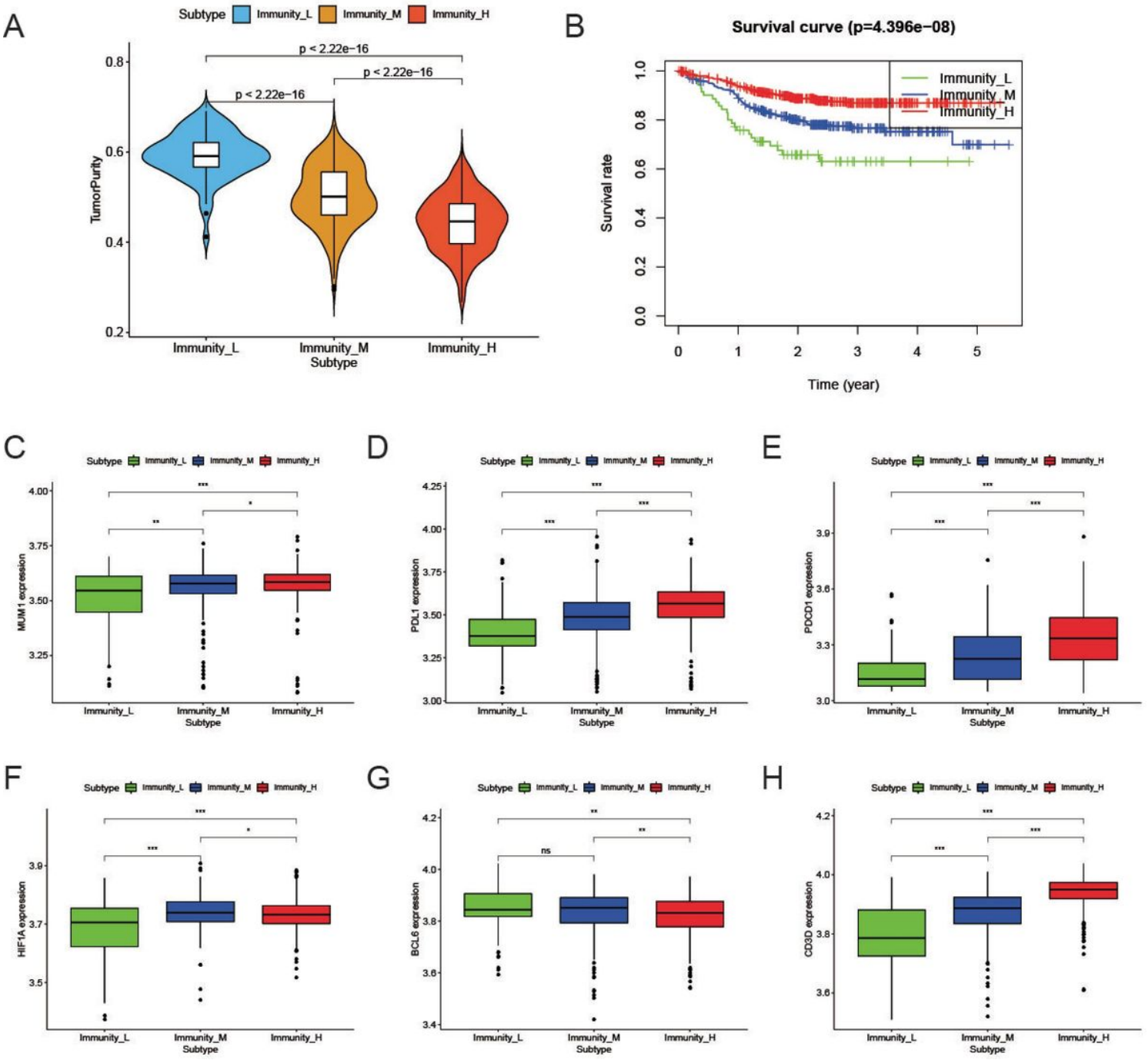

Figure 3

A: Analysis of differences in tumor purity between three immune subtypes. Tumor purity was importantly more down in Immunity_H group and importantly more excellent in Immunity_L (P <0.001, Kruskal-Wallis test). B: Survival analysis of three immune subgroups. The survival curves of Immunity_L, Immunity_M and Immunity_H subgroups were significantly different (P = 4.396E-08). It also proved that immune grouping had a good predictive effect on the survival of diffuse LARGE B-cell lymphoma. Patients in Immunity_H had the best prognosis, patients in Immunity_L had got the poorest prognosis, and the Immunity_M was between them. C-H: The expression of PD-1, PD-L1, CD3D, HIF1A, IRF4 and other genes was meaningfully correlated with the immune subgroup.The expressions of PD-1, PD-L1, CD3D, HIF1A,

IRF4 and other genes were meaningfully dissimilar between Immunity_L and Immunity_H (ANOVA text, P <0.001).

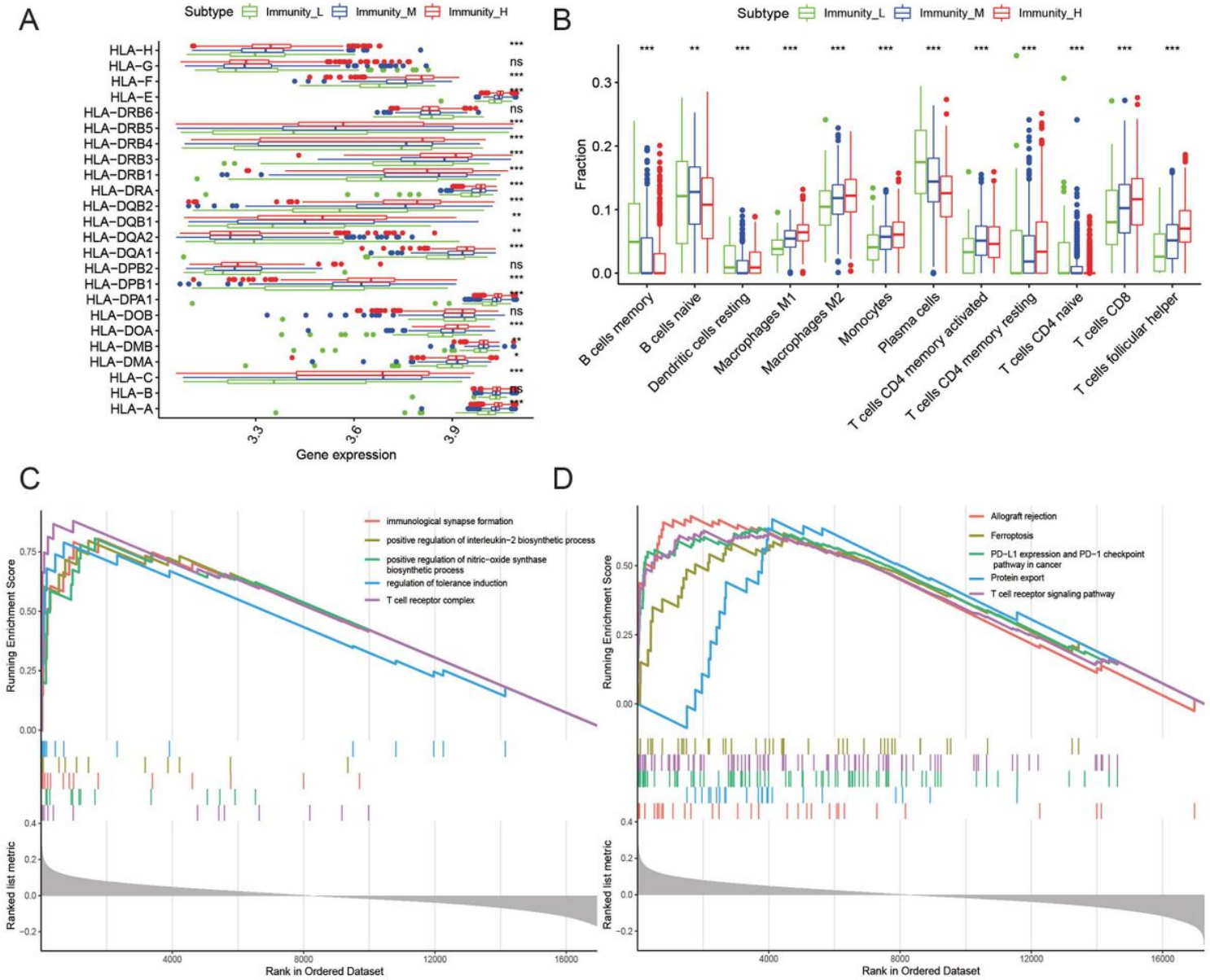

Figure 4

A : Immune subsets were significantly associated with HLA family genes. among 24 HLA-related genes, only five genes, HLA-G, HLA-DRB6, HLA-DPB2, HLA-DOB, and HLA-B, were not significant in the distribution of immune subsets. The remaining HLA family members were statistically distributed in the immune subgroups (p<0.06). B: Immune subtypes were significantly associated with immune cell infiltration.Monocytes, M1 Macrophages, M2 Macrophages, CD8+ T cells, CD4+ memory activated T cells and the follicular helper T cells were substantially high up in the Immunity_H group than in the Immunity_M groups and Immunity_L. The results of B cells naive, B cells memory, Plasma cells and CD4+ naive T cells in Immunity_L were considerably more excellent than those in Immunity_M and Immunity_H.

C-D: GO and KEGG analysis Differential gene enrichment analysis of Immunity_H and Immunity_L groups.

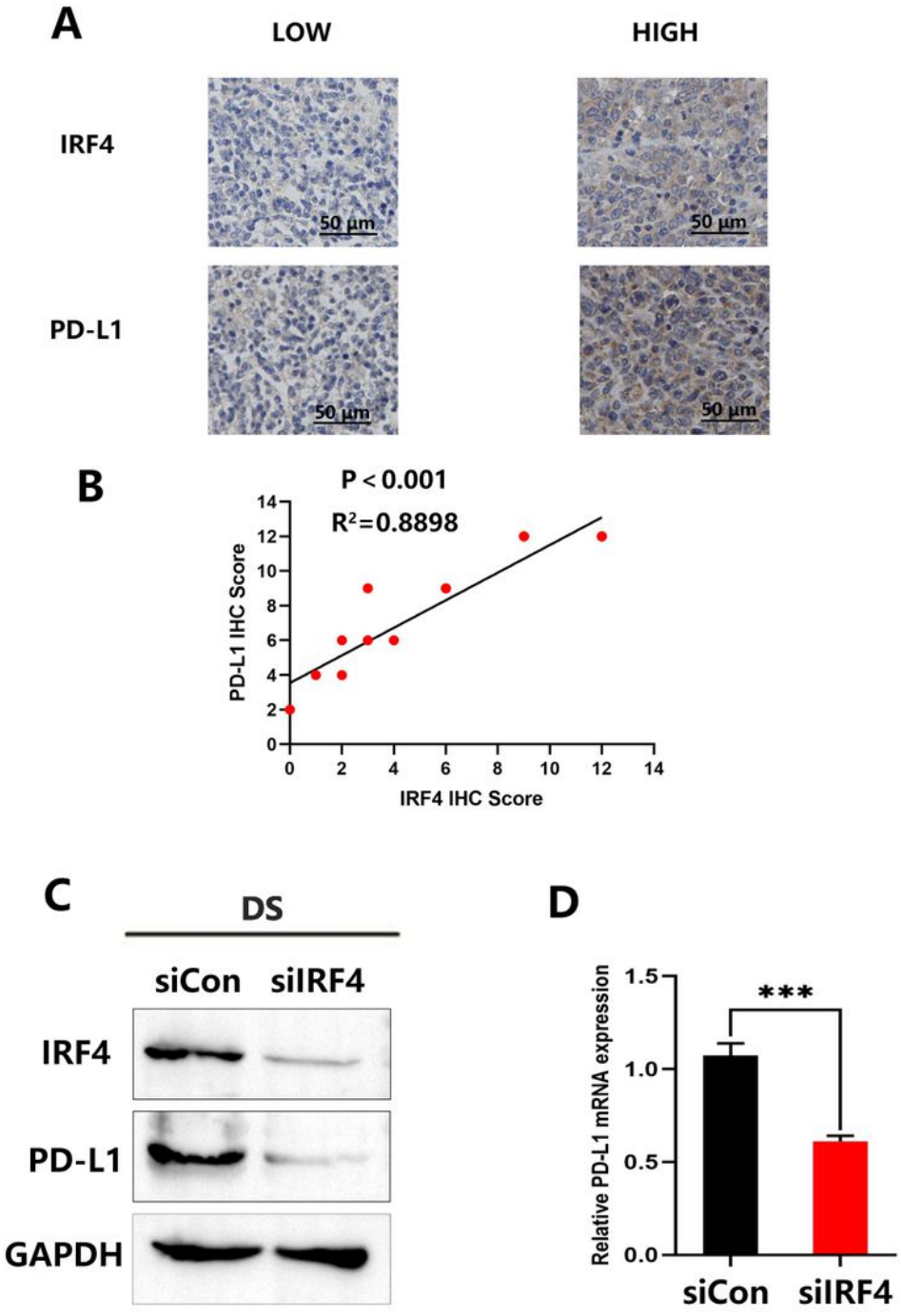

Figure 5

A: IHC was used to detect the expression of IRF4 and PD-L1 in DLBCL. Two cases were stained with IRF4 and PD-L1 immunohistochemistry.Examine the section under a microscope. B: The images described are

representative of 30 cases of DLBCL. Correlation between IRF4 IHC score and IRF4 IHC score in 30 DLBCL patients,calculated by Spearman's rank correlation methods, in 30 DLBCL cases. C: We transfected siControl and siIRF4 into DS cell line by transient transfection method. Proteins were collected and lysed, and the displayed proteins were analyzed by western blotting. D: The expression of PD-L1 was detected by real-time fluorescence quantitative PCR.The error bar represents three separate experiments.

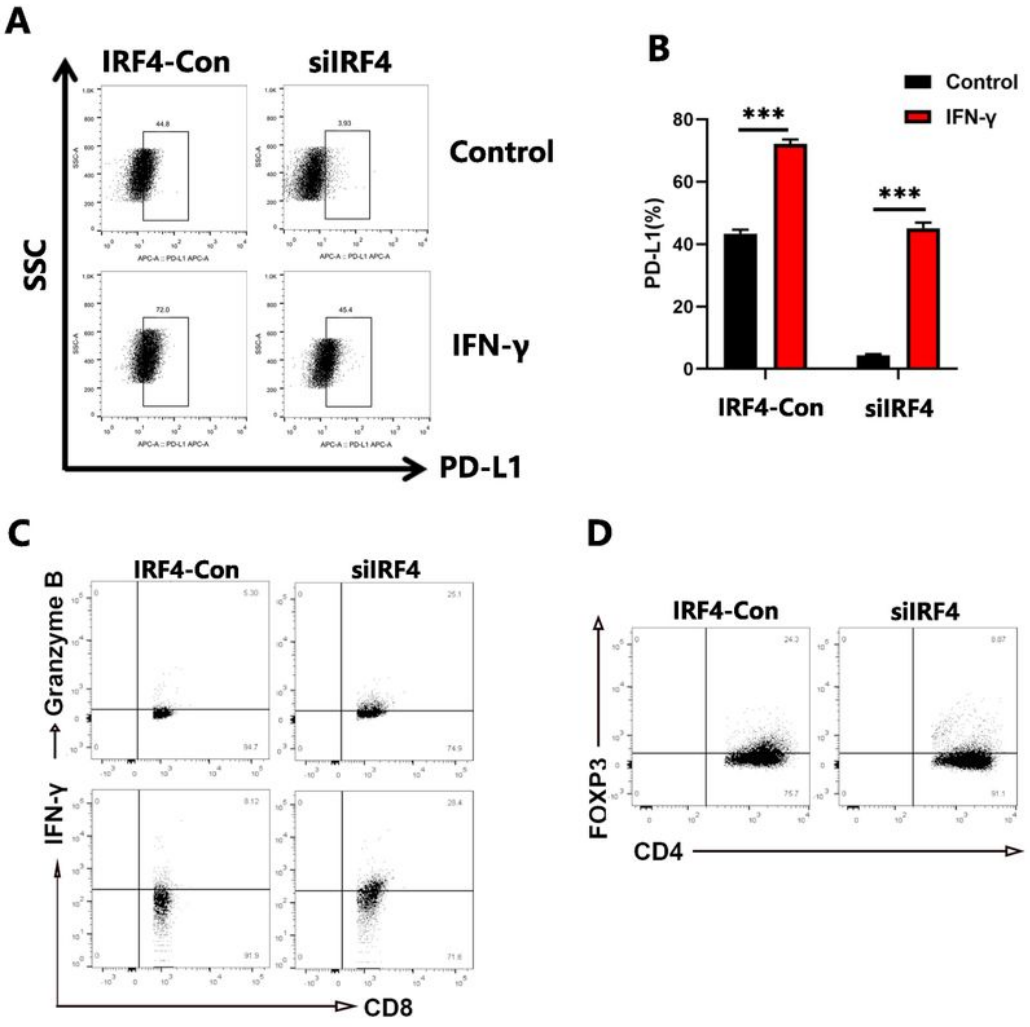

Figure 6

A-B: PD-L1's flow cytometry analysis in siIRF4 DS cells in relation to restriction with or without IFN-γ therapy. C: Flow cytometry was used to analyze GranzyB+ CD8+ T cell or IFN-γ+ CD8+ T cell frequencies. D: and CD4+T cell frequency or Treg(FOXP3) in the PBMC.

Supplementary Files

This is a list of supplementary files associated with this preprint. Click to download.

- Table1.pdf
- Table2.pdf